Polarized-Neutron Study of Spin Dynamics in the Kondo Insulator YbB_{12}

K. S. Nemkovski,[1] J.-M. Mignot,[2] P. A. Alekseev,[1] A. S. Ivanov,[3] E. V. Nefeodova,[1] A. V. Rybina,[1] L.-P. Regnault,[4] F. Iga,[5] and T. Takabatake[5]

[1]*LNSR, ISSSP, Russian Research Centre "Kurchatov Institute," 123182 Moscow, Russia*
[2]*Laboratoire Léon Brillouin, CEA-CNRS, CEA/Saclay, 91191 Gif sur Yvette, France*
[3]*Institut Laue-Langevin (ILL), B.P. 156, 38042 Grenoble Cedex 9, France*
[4]*DRFMC/SPSMS, CEA/Grenoble, 38054 Grenoble Cedex 9, France*
[5]*Department of Quantum Matter, ADSM, Hiroshima University, Higashi-Hiroshima 739-8530, Japan*

(Received 5 April 2007; published 26 September 2007)

Inelastic neutron scattering experiments have been performed on the archetype compound YbB_{12}, using neutron polarization analysis to separate the magnetic signal from the phonon background. With decreasing temperature, components characteristic for a single-site spin-fluctuation dynamics are suppressed, giving place to specific, strongly **Q**-dependent, low-energy excitations near the spin-gap edge. This crossover is discussed in terms of a simple crystal-field description of the incoherent high-temperature state and a predominantly local mechanism for the formation of the low-temperature singlet ground state.

DOI: 10.1103/PhysRevLett.99.137204 PACS numbers: 75.30.Mb, 71.70.Ch, 75.40.Gb, 78.70.Nx

In contrast to a majority of mixed-valence (MV) systems, which remain metallic down to very low temperatures and whose ground state can be described as a paramagnetic Fermi liquid, a small number of these materials evolve toward a semiconducting state with a relatively narrow gap on the order of 10 meV [1,2]. This gap typically opens with decreasing temperature in the range of $T^* \sim 100$ K and is accompanied by a drop in the magnetic susceptibility ascribed to the formation of a singlet ground state. Materials in this class, such as $Ce_3Bi_4Pt_3$ or YbB_{12}, are often termed ''Kondo insulators'' (KIs) because electronic correlations are thought to play a central role. The general form of their dynamical magnetic response at low temperature, as measured by inelastic neutron scattering (INS), is characterized by a spin gap, whose magnitude is comparable, though not necessarily equal, to the gap in the electronic density of states. In the cubic KI compound YbB_{12}, the magnetic signal at $T \approx 10$ K was indeed found to vanish at energies below $\sim$10 meV, but the response above the gap edge is not restricted to a smooth continuum. Neutron time-of-flight experiments on powder samples [3,4] have shown that it rather consists of three different peaks: two of them, $M1$ ($E \approx 15$ meV) and $M2$ (20 meV), are narrow, whereas the third one, $M3$ (38 meV), is considerably broader. With increasing temperature, a sizable quasielastic signal appears above $T = 50$ K. Above 100 K, the upper peak $M3$ is totally suppressed, and a single inelastic peak, hereafter denoted M_h, occurs at an energy of about 23 meV. Single-crystal measurements [5] have confirmed that the low-temperature peaks arise from distinct magnetic excitations, two of which ($M1$ and $M2$) exhibit significant dispersions in **Q** space. The energy of $M1$ has a pronounced minimum at the antiferromagnetic (AF) L point $\mathbf{q} = (\frac{1}{2}, \frac{1}{2}, \frac{1}{2})$, associated with a maximum in the intensity. In Ref. [5], this behavior was shown to be consistent with predictions for a spin exciton induced by AF correlations in a MV system with a hybridization gap [6]. Subsequently, high-resolution angle-resolved photoemission measurements [7] have shown the appearance, below $T \sim 60$ K, of an extra peak near 15–20 meV, localized in Q space around the L point, which was tentatively ascribed to indirect transitions across a hybridization gap. Also noteworthy is the clear evidence found, in a recent optical study [8], for coherence effects setting in for $T \lesssim 70$ K. However, some important issues have been left unsettled, among which are the connection between the single-site spin-fluctuation response at high temperature and the different spectral components observed in the spin-gap regime below T^*. In particular, it could not be decided whether $M2$ and the peak M_h occurring in the same energy range at high temperature were related or not, mainly because the magnetic signal could not be accurately separated from the large phonon background.

To shed light on this problem, we have carried out a comprehensive INS study of the magnetic response in YbB_{12} using polarized neutrons. Neutron polarization analysis makes it possible to separate the magnetic signal reliably over the entire Brillouin zone. The experiments were performed at the ILL in Grenoble on the triple-axis spectrometer IN20 (Heusler [111] monochromator and analyzer crystals). The sample studied (volume ≈ 0.4 cm^3) was the same as in Ref. [5]. It was oriented with a $\langle 110 \rangle$ crystal axis normal to the scattering plane and cooled to temperatures between 5 and 125 K inside an ILL-type He-flow cryostat. Neutron spectra were recorded at fixed final energy $E_f = 34.8$ meV, with a pyrolytic graphite filter placed in the scattered beam to remove higher-order contaminations but without Sollers collimators. All measurements were performed with the incident polarization $\mathbf{P}_0 \parallel \mathbf{Q}$, for which magnetic scattering occurs entirely in the spin-flip (SF) channel. The flipping ratio, as determined from the nuclear Bragg peak (004) of the sample, was

about 15. Data were recorded at $T = 5$ K for 13 inequivalent points in the Brillouin zone. Representative experimental SF spectra for different $\mathbf{Q}$ vectors are shown in Fig. 1. The contamination of SF spectra by non-spin-flip (NSF) processes, plotted as black dots in frames (a)–(c), is seen to be quite weak. We therefore chose to neglect it, as well as the weak SF contribution from incoherent nuclear-spin scattering, and to treat the SF signal as entirely magnetic. To extend the accessible energy range, data collected for larger equivalent Q vectors [$(\frac{3}{2}, \frac{3}{2}, \frac{5}{2})$ and $(0, 0, 3)$] have been combined to those plotted in Figs. 1(a) and 1(b) for $\mathbf{Q} = (\frac{3}{2}, \frac{3}{2}, \frac{3}{2})$ and $(1, 1, 2)$, respectively, after correcting them for the difference in form factors. This also produces an improvement of statistics in the region of overlap, as reflected by the error bars.

At the lowest temperature, the general form of the magnetic spectral response consists of three components, in agreement with previous measurements [3–5]. This is best evidenced by the spectrum measured at the L point

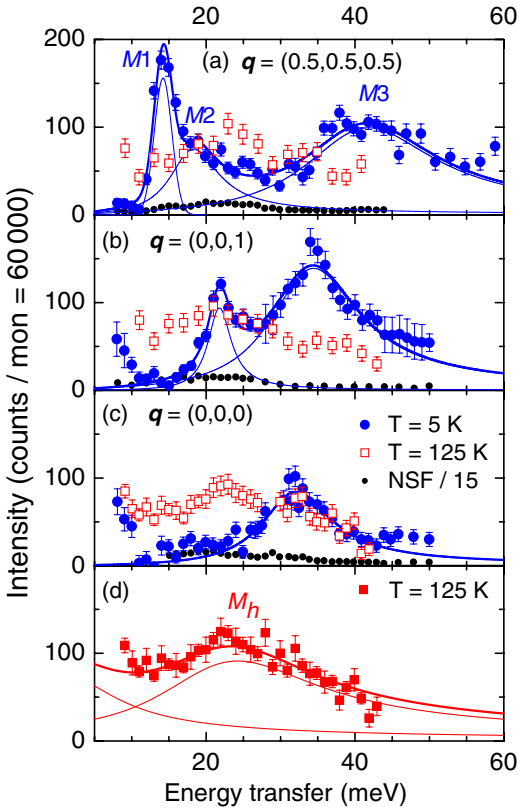

FIG. 1 (color online). Spin-flip neutron intensity (constant background subtracted) in YbB_{12} at $T = 5$ (circles) and 125 K (squares) corresponding to the (a) L, (b) X, and (c) Γ points; black dots: non-spin-flip signal divided by the polarization ratio (NSF contamination in the SF channel); thick (thin) lines: total (partial) intensities from the fits. (d): Average of the L-, X-, and Γ-point spectra for $T = 125$ K (intensities in this frame are scaled to $Q = 0$ according to the Yb^{3+} magnetic form factor prior to averaging). The upturns at energies below 10 meV seen for some Q vectors [(b),(c)] occur in both the SF and the NSF channels and are due to higher-order Bragg contaminations.

[Fig. 1(a)], in which the three peaks $M1$, $M2$, and $M3$ exist together, with sizable intensities, at energies of 14.1, 17.9, and 40.4 meV, respectively. All excitations are dispersive, and their intensities and linewidths vary significantly with $\mathbf{q}$ as shown in Fig. 2. The values plotted here, as well as the solid lines in Fig. 1, were derived from the same fitting procedure described in Ref. [5]. The L point corresponds to a minimum in the dispersions of both $M1$ and $M2$. Moving from L to X along the zone boundary, $M1$ is gradually suppressed, while $M2$ becomes narrower. The upper peak $M3$ shifts to lower energies, with a steady decrease in its linewidth. At the zone center, $M1$ and $M2$ disappear, and the only remaining magnetic component is $M3$.

For $M1$, the present data confirm the $\mathbf{Q}$ dependence derived from unpolarized neutron data [5], supporting the phonon subtraction procedure applied in the latter study. Both data sets were therefore combined in order to improve the mapping of $M1$ in $\mathbf{Q}$ space. The result, shown in Fig. 3(a), confirms that the intensity has a rather broad maximum near the L point, which also corresponds to the absolute minimum in the dispersion (upper frame in Fig. 2). It is therefore reasonable to ascribe $M1$ to AF correlations at the wave vector $\mathbf{k} = (\frac{1}{2}, \frac{1}{2}, \frac{1}{2})$, as argued in Ref. [5]. The polarized-neutron data indicate that $M1$ has no measurable intensity at the zone center and along the Γ-X line [$\mathbf{q} = (0, 0, \zeta)$]. They further reveal that the energy and intensity of $M1$ remain practically constant along the $(\frac{1}{2}, \frac{1}{2}, \zeta)$ line [ridge of intensity parallel to [001] going through the L point in Fig. 3(a)], suggesting a significant 2D character of the fluctuations associated with $M1$.

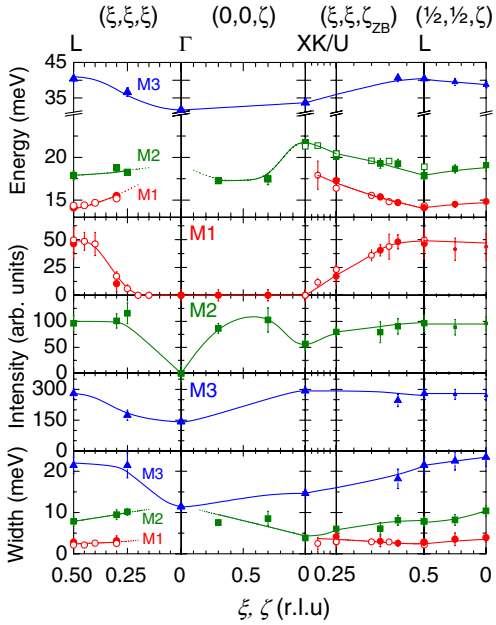

FIG. 2 (color online). $\mathbf{q}$ dependence of peak energies, integrated intensities, and experimental peak widths for the three magnetic excitations $M1$ (circles), $M2$ (squares), and $M3$ (triangles) at $T = 5$ K; solid (open) symbols represent data from this study and Ref. [5], respectively; lines are guides to the eye.

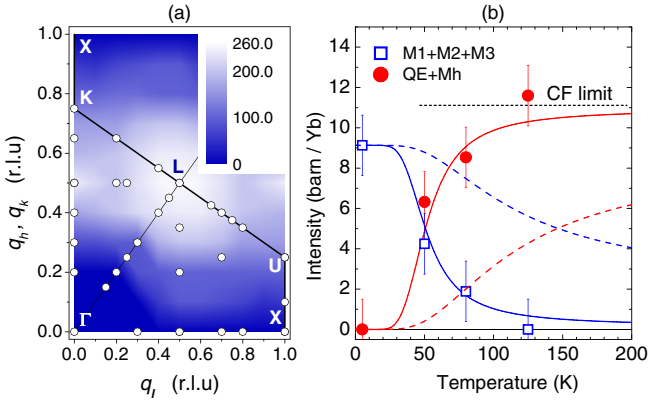

FIG. 3 (color online). (a) Intensity map at $T = 5$ K for $M1$ over one quadrant of the Brillouin zone; circles denote **Q** vectors at which energy spectra have been measured. (b) Temperature dependence of the partial cross sections at the L point; open squares: sum of $M1$, $M2$, and $M3$; solid circles: sum of the quasielastic and high-temperature (M_h) components; solid and dashed curves: calculation (see text); dotted line: Yb^{3+} CF cross section.

Assuming the intensity distribution to reflect the range of AF interactions between Yb moments, we have estimated correlation lengths perpendicular and parallel to the above direction, corresponding, respectively, to couplings within ($\xi_\parallel$) or between ($\xi_\perp$) the (001) planes. Despite sizable statistical uncertainty, the values obtained, $\xi_\parallel = 5.4 \pm 1.4$ Å and $\xi_\perp = 3.4 \pm 1.1$ Å, confirm the anisotropy already visible in the figure.

The second mode $M2$ is broader in energy than $M1$ and has stronger integrated intensity but behaves qualitatively similar to $M1$ over most of the Brillouin zone. The main difference is found along the $(0, 0, \zeta)$ direction, where the intensity of $M2$ does not vanish, except at the Γ point. Surprisingly, a considerable loss of intensity occurs near the X point owing to a decrease in the peak *width* [9].

$M3$ is the only magnetic excitation that exists over the entire Brillouin zone, including the zone center. It was previously ascribed to single-site effects, mainly because experiments on $Yb_{1-x}Lu_xB_{12}$ alloys [10,11] showed no pronounced influence of rare-earth dilution. This assumption is not supported by the pronounced **q** dependence observed in the present experiment, and the insensitivity to disorder is thus more likely due to the large intrinsic width of the $M3$ peak. As can be seen in Fig. 2, the largest intensity is again found at the L point and along the $(\frac{1}{2}, \frac{1}{2}, \zeta)$ line, but, in contrast to $M1$ and $M2$, the energy decreases from the L point, both in the L-Γ direction and along the zone boundary.

At the highest temperature in this experiment $T = 125$ K $> T^*$, all SF spectra measured at different **Q** vectors were found to coincide within error bars (Fig. 1). In agreement with the results of previous powder experiments, they consist of one broad quasielastic (QE) peak and a single inelastic peak (M_h) just above 20 meV. In order to improve statistics, all spectra were thus combined together, yielding the result shown in Fig. 1(d). The observed absence of **q** dependence indicates that the magnetic response in this temperature range arises primarily from single-site processes. At the Γ point, cooling down to $T = 5$ K results in the suppression of M_h together with the QE signal. This clearly demonstrates that M_h cannot be connected with either $M1$ or $M2$ becoming dispersionless at high temperature. The most consistent fitting of spectra at intermediate temperatures is actually achieved by assuming that the Q dependence of M_h and of the QE peak is entirely due to that of the magnetic form factor. Finally, the overall temperature evolution is the same for all **Q** vectors; namely, the low-temperature spin-gap response with strongly **Q**-dependent collective excitations is replaced by a single-site response. In this process, the three peaks $M1$–$M3$ are suppressed rather steeply, while new spectral components appear. This behavior is clearly evidenced in Fig. 3(b), where the integrated intensities derived from the fits for $[M1 + M2 + M3]$ and for $[M_h + \mathrm{QE}]$ are plotted as a function of temperature [12].

As noted above, the magnetic response at $T = 125$ K is single-site, and its shape is similar to that encountered in other metallic MV compounds. It is therefore natural to consider first a simple interpretation based on crystal-field (CF) effects. A plausible, though indirect, determination of the CF potential in YbB_{12} was obtained previously by using Er^{3+} impurities as a local probe [10]. The total splitting of the spin-orbit multiplet $^2F_{7/2}$ for Yb^{3+} in the absence of a valence instability was estimated to be on the order of 10 meV, with a ground state quartet Γ_8 and two excited doublets Γ_7 and Γ_6. The values calculated for the above level scheme are $\sigma_{\mathrm{QE}} = 2.88$ b (sum of the $\Gamma_8 \rightarrow \Gamma_8$, $\Gamma_7 \rightarrow \Gamma_7$, and $\Gamma_6 \rightarrow \Gamma_6$ cross sections), $\sigma_{\Gamma_8 \rightarrow \Gamma_7} = 3.59$ b, and $\sigma_{\Gamma_8 \rightarrow \Gamma_6} = 4.65$ b. Absolute calibration of the experimental intensities can be achieved by scaling our high-temperature spectra to the results of a previous time-of-flight experiment on powder samples [4]. The resulting cross sections are $\sigma_{\mathrm{QE}} = 3.52 \pm 0.82$ b for the QE peak and $\sigma_{\mathrm{inel}} = 8.07 \pm 1.2$ b for the M_h peak. The agreement with the calculation is fairly good if we ascribe the inelastic component M_h to transitions from Γ_8 to both Γ_7 and Γ_6. This supposes that, because of $f - d$ hybridization ($T_K \sim 90$ K, as estimated from $\Gamma_{\mathrm{QE}}/2 \approx 8$ meV), the CF levels have shifted and/or broadened so as to become undistinguishable. Such renormalization been reported for systems with f-electron instabilities such as $CeAl_3$ [13], $CeCu_6$ [14], or $YbNi_2B_2C$ [15], in which the quasielastic response is accompanied by a broad inelastic peak originating from CF transitions, and might occur in YbB_{12} as well.

The spin-gap response observed in Kondo insulators at temperatures lower than T^* is often interpreted in terms of indirect electron-hole excitations across a hybridization gap [2]. In the case of YbB_{12}, this view has recently received support from optical measurements, in which a conductivity onset in $\sigma(\omega)$ was found at about 15 meV [16], very close to the value of the spin-gap energy. On the

other hand, the persistence of the spin gap in $Yb_{1-x}Lu_xB_{12}$ to a high level of dilution [10] seems to be more in favor of a local mechanism [17,18]. In the model proposed by Liu [18], the ground state is represented as a lattice of localized spin singlets obtained by the superposition of the $4f^{14}$ and $4f^{13}5d^1$ states of Yb. Because of the degeneracy of the lowest $4f^{13}$ multiplet ($J = 7/2$), the excited levels are comprised of eight one-hole states hybridized with the d conduction band. Assuming these levels to be split by the crystal field, and based on the above analysis of the high-temperature spectra, one could ascribe $M2$ and $M3$, respectively, to transitions from the singlet ground state to the Γ_8 and the $\Gamma_7 - \Gamma_6$ excited states. The larger width of $M3$ may reflect a small energy difference between Γ_7 and Γ_6. The lower edge of $M2$ defines the position of the spin gap, and $M1$ thus represents an in-gap, resolution-limited, excitonlike mode, in line with the interpretation of Ref. [5]. For a purely single-site mechanism, any $\mathbf{q}$ dependence observed experimentally has to be ascribed to dispersion taking place in both the valence and the conduction bands. In the real system, however, additional effects due to exchange interactions $\mathcal{J}_{i,j}$ between Yb neighbors may affect the behavior of $M2$ and $M3$. As to $M1$, if this mode actually corresponds to a spin exciton, its dispersion should reflect the $\mathbf{q}$ dependence not only of the spin gap but also of $\mathcal{J}(\mathbf{q})$. Experimentally, the dispersion of $M1$ is similar to that of $M2$ taken to represent the gap edge but goes through a more pronounced minimum at the L point, which may be the fingerprint of AF correlations.

With increasing temperature, the most striking effect in the spin dynamics of YbB_{12} is the rapid recovery of the incoherent regime at temperatures significantly below the energy of the spin gap [3,4], as illustrated by the intensities plotted in Fig. 3(b). This behavior is at variance with the calculations of Ref. [18], which predict the quasielastic component to remain weak up to temperatures on the order of 150 K. Simple thermal population effects for a singlet ground state and a g-fold degenerate excited state fail to represent the steepness of the observed dependence [dashed curves in Fig. 3(b) for $g = 4$, corresponding to the degeneracy of the lowest CF level], unless by assuming unrealistically large g values (solid curves obtained for $g = 80$). This stresses the need for a microscopic description of how the many-body singlet ground state characteristic for Kondo insulators evolves from the high-temperature degenerate level scheme dictated by Kramers theorem in the single-site regime. Interestingly, similar questions arise from a recent study of dispersive magnetic excitations in the *metallic* spin-gap MV compound $YbAl_3$ [19].

In summary, the present study provides a reliable experimental basis to assess the spin dynamics in YbB_{12} by ensuring proper separation of the nonmagnetic background from neutron polarization analysis. In the high-temperature regime, single-site fluctuations dominate, and the magnetic response is consistent with a simple damped crystal-field excitation spectrum. At low temperature, a spin-gap response develops in the Kondo insulator state and new dispersive excitations appear. Following the suggestion from dilution experiments that local effects play a leading role in the formation of this new ground state, it is shown that a description based on an array of singlet states can qualitatively account for the general form of the spectra. In this interpretation, the sharp excitation $M1$ occurring at 15 meV is tentatively ascribed to a spin-exciton mode stabilized by AF correlations between Yb sites. Since this feature was originally derived in an coherent hybridization-gap approach, further theoretical work is now needed to see how it might be applicable in a more local situation.

We are grateful to V. N. Lazukov, N. N. Tiden, B. Dorner, N. M. Plakida, Yu. M. Kagan, and I. P. Sadikov for stimulating discussions and M. Enderle and J. Kulda for their help during the experiments. The work was supported by RFBR Grant No. 05-02-16426.

[1] T. Takabatake *et al.*, J. Magn. Magn. Mater. **177–181**, 277 (1998).
[2] P. S. Riseborough, Adv. Phys. **49**, 257 (2000).
[3] A. Bouvet, Thèse de Doctorat, University of Grenoble, 1993; A. Bouvet *et al.*, J. Phys. Condens. Matter **10**, 5667 (1998).
[4] E. V. Nefeodova *et al.*, Phys. Rev. B **60**, 13 507 (1999).
[5] J.-M. Mignot *et al.*, Phys. Rev. Lett. **94**, 247204 (2005).
[6] P. S. Riseborough, J. Magn. Magn. Mater. **226–230**, 127 (2001).
[7] Y. Takeda *et al.*, Phys. Rev. B **73**, 033202 (2006).
[8] B. Gorshunov *et al.*, Phys. Rev. B **73**, 045207 (2006).
[9] In the case of $M1$, it would not be possible to observe such an effect because the peak is resolution-limited and gives essentially no information as to the intrinsic damping of the mode.
[10] P. A. Alekseev *et al.*, J. Phys. Condens. Matter **16**, 2631 (2004).
[11] E. Nefeodova *et al.*, J. Solid State Chem. **179**, 2858 (2006).
[12] To ensure consistent fitting of the magnetic spectra at different temperatures, the linewidths for M_h and the QE peak were fixed to the values from powder measurements [4]. The latter data were first reanalyzed using the information that $M2$ and M_h are distinct excitations, thus letting the M_h linewidth increase at the expense of the QE one.
[13] P. A. Alekseev *et al.*, Physica (Amsterdam) **217B**, 241 (1996).
[14] E. A. Goremychkin and R. Osborn, Phys. Rev. B **47**, 14 580 (1993).
[15] A. T. Boothroyd *et al.*, Phys. Rev. B **67**, 104407 (2003).
[16] H. Okamura *et al.*, J. Phys. Soc. Jpn. **74**, 1954 (2005).
[17] T. Kasuya, Europhys. Lett. **26**, 277 (1994).
[18] S. H. Liu, Phys. Rev. B **63**, 115108 (2001).
[19] A. D. Christianson *et al.*, Phys. Rev. Lett. **96**, 117206 (2006).